



Affect of Spatial and Temporal Discretization in the Numerical Solution of One-Dimensional Variably Saturated Flow Equation

By M. S. Islam & R. Ahamad

Abstract- Numerical simulation of the Richards' equation in dynamically saturated soils keeps on being a difficult assignment because of its highly non-linear course of action. This is especially evident as soils approach saturation and the conduct of the principal partial differential equation changes from elliptic to parabolic. In this study, we developed a numerical model for solving Richards' equation with regards to finite element approach in which pressure head-based scheme is proposed to approximate the governing equation, and mass-lumping techniques are used to maintain stability of the numerical simulation. Dynamic adaptive time stepping procedure is implemented in the Picard and Newton linearization schemes. The robustness and accuracy of the numerical model were demonstrated through simulation of two difficult tests, including sharp moisture front that infiltrates into the soil column with time dependent boundary condition and flow into a layered soil with variable initial conditions.

Keywords: *richards' equation; finite element; variably saturated flow; spatial discretization; temporal discretization.*

GJSFR-F Classification: MSC 2010: 37M15



AFFECT OF SPATIAL AND TEMPORAL DISCRETIZATION IN THE NUMERICAL SOLUTION OF ONE-DIMENSIONAL VARIABLY SATURATED FLOW EQUATION

Strictly as per the compliance and regulations of:



RESEARCH | DIVERSITY | ETHICS



Affect of Spatial and Temporal Discretization in the Numerical Solution of One-Dimensional Variably Saturated Flow Equation

M. S. Islam ^a & R. Ahamad ^a

Abstract- Numerical simulation of the Richards' equation in dynamically saturated soils keeps on being a difficult assignment because of its highly non-linear course of action. This is especially evident as soils approach saturation and the conduct of the principal partial differential equation changes from elliptic to parabolic. In this study, we developed a numerical model for solving Richards' equation with regards to finite element approach in which pressure head-based scheme is proposed to approximate the governing equation, and mass-lumping techniques are used to maintain stability of the numerical simulation. Dynamic adaptive time stepping procedure is implemented in the Picard and Newton linearization schemes. The robustness and accuracy of the numerical model were demonstrated through simulation of two difficult tests, including sharp moisture front that infiltrates into the soil column with time dependent boundary condition and flow into a layered soil with variable initial conditions. The two cases introduced feature various parts of the presentation of the two iterative strategies and the various components that can influence their convergence and efficiency, spatial and temporal discretization, convergence error norm, time weighting, conductivity and moisture content attributes and the degree of completely saturated regions in the soil. Numerical accuracy, mass balance nature and iteration efficiency of Picard and Newton techniques are compared using different step sizes and spatial resolutions. Results demonstrated that the presented algorithm is vigorous and exact in simulating variably saturated flows and outcomes of some hydrologic process simulations are affected significantly by the spatial and temporal grid scales. Hence it is proposed that the strategy can be adequately actualized and used in numerical models of Richards' equation.

Keywords: richards' equation; finite element; variably saturated flow; spatial discretization; temporal discretization.

I. INTRODUCTION

Ground water flow issues are moderately hard to solve because of their nonlinear and parabolic nature, dependent on space and time dependent boundary conditions, nonhomogeneous parameters, etc. Analytical solution can once in a while be acquired for such genuine frameworks. In this way much of the time, flow equations must be illuminated by numerical approximations. However, numerically solving the flow problem is regularly tested by numerical scattering and motions, and as often as possible winds up with misleading outcomes. Inexact results of numerical approximations might be a significant reason for much disarray in the quantifiable analysis of flow problems.

Author a a: Department of Mathematics, Shahjalal University of Science & Technology, Sylhet, Bangladesh.
e-mail: sislam_25@yahoo.com

1. Miller, C. T., Williams, G. A., Kelly, C. T., and Tocci, M. D.: *Robust solution of Richards' equation for nonuniform porous media*. Water Resour. Res., 1998, 34:2599-2610.

Existing numerical methodologies to deal with explain Richards' equation vary by the detailing of this equation, for example, grid discretization, time step and resolution strategies. These decisions impact computational time, numerical strength and result exactness. Numerical strategies for Richards' equation have pulled in extensive examination consideration and are generally utilized in reasonable simulations of subsurface procedures. In any case, numerous examinations have been indicated that standard numerical process cannot overcome difficulties for certain flow problems satisfactorily, particularly for the saturation of at first dry soils with non-uniform pore size appropriation [1]. This examination researches the upsides of noniterative adaptive time stepping approximations for Richards' equation and built up a simple cost-effective approximation that takes care of these troublesome issues precisely. The proposed formulation is firmly identified with in backward Euler techniques and henceforth can be utilized to progress existing programming for pragmatic subsurface simulations.

Standard numerical strategies for Richards' equation is principally restricted to straightforward time stepping approximations combined with finite element or finite difference spatial approximations [2]. The time stepping approximations included backward Euler and related schemes [e.g., 3, 4]. A basic advancement in the numerical examination of Richards' equation is the presentation of adaptive time stepping algorithms, which acclimate to the conduct of the solution and are commonly more solid and productive than uncontrolled procedures. Adaptive spatial approximations for Richards' equation incorporate a hierarchic finite element technique [5] and a front-tracking scheme [6].

Variable-order variable-step size differential algebraic equation solvers (DASPK) [1, 7, 8], lower-order backward Euler and similar techniques [9, 10] are depicted and successfully applied in the pressure head form of Richards' equation. Modern high-order techniques gave significant upgrades over existing low-order uniform step-size procedures when a small tolerance is used. In any case, for practical framework, many ordinary differential equation algorithms have certain constraints in the modeling variably saturated flows. By the controlling of formal truncation error, impressive improvements in solution accuracy and efficiency are achievable using fixed step and heuristic time stepping approximations, as well as, enhances the mass balance of models dependent on pressure head form of Richards' equation.

A significant issue in taking care of the flow problem is the mass balance error relating to its nonlinear nature when flow includes physical and chemical responses, for example, degradation, adsorption, evapotranspiration, and production. Mass preservation is an important obligation for accurate numerical solution, while, numerical accuracy is not ensured with a small mass balance. Iterative solution techniques with small step size can reduce the mass balance error, which thus makes the solution procedures very expensive. Numerical encounters for certain cases, contingent upon the nature and level of the nonlinearity, shows that mass balance errors may not be adequately wiped out in any event, when small steps are utilized. Thus, in flow demonstrating, most consideration has been paid to overcoming nonlinearity and eliminating the numerical scattering and false motions of the flow problems.

The governing equation for flow in saturated porous media i.e., Richards' equation, contains nonlinearities arising from pressure head dependencies on soil moisture and hydraulic conductivity. For steadiness reasons an implicit time discretization requiring assessment of the nonlinear coefficients at the current time level, is typically used to tackle the equation numerically. To linearize the subsequent discrete

system of equations, Newton or Picard method is ordinarily utilized numerical techniques for solving the nonlinearity of the coupled system [3, 11]. Newton-Krylov method, combined Picard-Newton method, initial slope Newton methods are also used to solve Richards' equation [12, 13, 14]. Basically, Picard scheme is the most famous because of its straightforwardness and normally adequate performance [15], and, is computationally more affordable on a for each iteration premise, and preserves symmetry of the discrete system of equations. Yet, the technique may diverge under specific conditions, as has been watched experimentally [3]. Furthermore, the non-perfection of constitutive relationships depicting a few soils causes poor convergence or complete divergence of Picard and Newton solvers for uncontrolled time stepping algorithms. To enhance the convergence efficiencies for such difficult simulations, improved sophisticated variable-order variable-step size strategies along chord slope iteration integrator and Newton techniques with global line search method can be employed [1, 7]. The Newton technique, yields nonsymmetric system matrices and is more unpredictable and costly than Picard linearization, however it accomplishes a higher rate of convergence and can be more strong than Picard for particular sorts of issues. Utilization of the Newton method has been restricted to one-and two-dimensional saturated-unsaturated flow models. Detail comparison of Picard and Newton strategies has been directed for the transient one-dimensional Richards' equation is found in the study [3], where it was demonstrated that, regarding CPU time expected to accomplish a given degree of solution exactness, Newton scheme can be as or more effective than Picard.

The number of iterations are expected to converge is a deciding component in the linearization schemes such as the Picard and Newton for the accurate, robust and efficient simulations. Therefore to meet this rationale, convergence rate is often enhanced by providing the solver with an initial solution estimate that is closer to the final solution for the current time step. This can be obtained by taking the initial guess from the previous step and by choosing a sufficiently small time step [13]. Hence, empirical dynamic adaptive time step criterion is required for a numerical model [3, 13, 16, 17].

Possible efficiency advantages can be obtained by use of noniterative schemes where formation of a single matrix with inversion per time step is required. For instance, the study [3] demonstrated that the noniterative implicit factored scheme with Newton solver can display equivalent or higher convergence efficiency than Crank-Nicolson method. However, it is not comfortable to handle the Richards' equation, as well as, much complexities are occurred at the saturated-unsaturated interface. Besides, these simpler algorithms, noniterative linearizations are limited for the temporal accuracy to first order. Regardless of these complexities, noniterative linearization techniques are an alluring option in contrast to customary iterative techniques for solving Richards' equation and other nonlinear partial differential equations.

The goal of this study, a general head-based mass conservative numerical procedure with regards to finite element scheme is developed to approximate the governing equation in which mass-lumping strategies are utilized to keep the stability of numerical simulation. To investigate the applicability and accuracy of the mathematical model and solution technique that offers a stable solution without requiring the resizing of the finite element mesh structure. To analyze complete flow behavior, realistic initial and Dirichlet boundary conditions are imposed in the numerical simulator to the head-based form of Richards' equation. Adaptive time-stepping approach is employed to minimize the computational time and maintain small truncation error. The performance

II. GOVERNING EQUATIONS

of the algorithm is shown to be superior to the conventional pressure head-based form and can easily be used in layered soil.

Notes

Move through fluidly saturated permeable media is portrayed by the classical Richards' equation, which is joined by coupling an announcement of mass preservation with the Darcy's equation. Richards' equation contains nonlinearities emerging from pressure head conditions in the soil moisture and hydraulic conductivity. For settling Richards' equation utilizing regular numerical techniques can prompt a progression of numerical troubles including loss of mass protection, inadequately settled sharp fronts, and disappointment for nonlinear solver or iterative linear solvers. Also, precise and effective simulation of ground water flow in the saturated-unsaturated zone is computationally pricey, particularly for issues those are described by sharp fronts in both realities. Normal calculations that utilize homogeneous spatial and transient discretizations for the numerical solution of these issues lead to off base, wasteful, some time shaky and costly simulations. To evade these numerical challenges, mass-preservation plan of flow condition, fine discretization in reality can be utilized, and need to usage of proficient solid nonlinear and linear calculations. While bringing about solutions of adequate precision, these methodologies can be computationally costly, particularly when simulating conditions that include sharp fronts in space and timey, time varying boundary conditions, vertical redistribution, just as various soil materials in flow system.

Richards' equation might be written in three standard structures, with either pressure head or moisture content as dependent variables. The constitutive connection between fluid substance and pressure head takes into account transformation of one type of the condition to another. Three standard types of the saturated-unsaturated flow condition might be distinguished by the ' ψ -based', ' θ -based', and the 'mixed (ψ - θ)' form. For one-dimensional vertical flow, these conditions can be composed as follows:

(i) The ' ψ -based' form, where the primary variable is the pressure head,

$$C(\psi) \frac{\partial \psi}{\partial t} = \frac{\partial}{\partial z} \left[K(\psi) \left(\frac{\partial \psi}{\partial z} + 1 \right) \right] \quad (1)$$

where, $C(\psi)$ is the specific fluid capacity $[L^{-1}]$ and is defined by $C(\psi) = \frac{d\theta}{d\psi}$, ψ is the pressure head $[L]$, t is time $[T]$, z denotes the vertical distance from reference elevation, assumed positive upward $[L]$, $K(\psi)$ is the hydraulic conductivity $[LT^{-1}]$, and θ is the moisture content.

The ' ψ -based' form permits for both unsaturated and saturated conditions. However, in highly non-linear problems, such as infiltration into very dry heterogeneous soils, these methods can suffer from mass-balance error, convergence problems and poor CPU efficiency. The reason for poor mass balance resides in the time derivative term.

While $\frac{d\theta}{dt}$ and $C(\psi) \left(\frac{d\psi}{dt} \right)$ are mathematically equivalent in the continuous partial differential equation, their discrete analogues are not. The inequality in the discrete forms is exacerbated by the highly nonlinear nature of the specific capacity term $C(\psi)$. This leads to significant mass-balance errors in the ψ -based formulations because the change in mass in the system is calculated using discrete values of $\frac{d\theta}{dt}$ while the

approximating equations use the expansion $C(\psi) \left(\frac{d\psi}{dt} \right)$. Using standard time-integration techniques, mass-balance errors grow with the time-step size. Various approaches have been developed to overcome this problem. A mass-conserving solution that modifies the capacity term to force global mass balance scheme is proposed [18]. A mass distributed algorithm [19] that satisfied mass balance and was free from oscillation. Implementation of method of lines is shown the property of good mass balance through time-step truncation error [7]. Moreover, very fine spatial and temporal discretizations with mass lumping are needed to maintain mass balance property for these scenarios.

(ii) The θ -based form, where the primary variable is the moisture content,

$$\frac{\partial \theta}{\partial t} = \frac{\partial}{\partial z} \left[D(\theta) \frac{\partial \theta}{\partial z} \right] + \frac{\partial K}{\partial z} \quad (2)$$

where $D(\theta) = \frac{K}{C(\psi)} = K \frac{d\psi}{d\theta}$ is the soil water unsaturated diffusivity [$L^2 T^{-1}$]. One of the advantages of the θ -based formulation is that perfectly mass conservative discrete approximations can be applied. However, this form degenerates under fully saturated conditions as heterogeneous material produces discontinuous θ profiles and a pressure-saturation relationship no longer exist [20]. Thus, this form may be useful only for homogeneous porous media.

(iii) The mixed form, where both θ and ψ are the dependent variables,

$$\frac{\partial \theta}{\partial t} = \frac{\partial}{\partial z} \left[K(\psi) \left(\frac{\partial \psi}{\partial z} + 1 \right) \right] \quad (3)$$

It is also expressed in terms of mass conservative formulation. This form can be used to solve for both saturated-unsaturated flow cases. It is commonly viewed as better than the other two structures as a result of vigor as for mass balance. However, conservation of mass alone does not guarantee satisfactory numerical solutions [4, 21]. Numerical strategies that utilize both θ and ψ in the solution system have been developed to reduce the mass balance errors and improve computational efficiency. A primary variable switching technique, which is unconditionally mass conservative [22]. This method involves assembling and solving a nonsymmetric equation system at each time and iteration level which increases CPU time but reported faster convergence behavior. Modified Picard iteration approach guarantees mass balance by assessing the moisture content change in a period step legitimately from the adjustment in the water pressure head [4]. It has been shown to provide excellent mass balance when modelling unsaturated problems with sharp wetting fronts [23]. This method is easy to implement into ψ -based codes, requiring only an additional source term.

More efficient convergence scheme has been proposed for the modified Picard iteration method dependent on utilizing the pressure head as the primary variable [24]. However, problems have been reported when employing the mixed form for free drainage problems [25]. If relatively large values are encountered, mass-balance errors can accumulate with longer simulation times and larger domains. The ψ -based form can achieve good mass balance if the change in ψ is small enough during a time step whereas the mixed form improves mass balance with a sharp wetting front. Therefore, combining these, makes a more efficient procedure for long time simulations of water flow in soils with frequent infiltration and deep drainage processes. The method switches to the ψ -based form when the change in ψ is less than some prescribed value, otherwise the mixed form is applied. Developing robust and efficient algorithms for

certain flow problems, such as those that give rise to sharp wetting fronts, has provided a computational challenge to the simulation community. For this class of problem, small time-step sizes and a fine mesh is often required in order to maintain stability when steep wetting fronts develop, making large-scale multi-dimensional infiltration problems impractical to simulate.

a) *Constitutive Relationships*

For solving Richards' equation numerically, we must define the characteristic functions to illustrate the relationship among fluid pressures, saturations and relative permeabilities. Various mathematical formulations are used in modeling for the soil water moisture curves. The most regularly utilized connections are the Brooks–Corey [26] and the van Genuchten [27] models. These two models are described as follows:

i. *Brooks–Corey Model*

The soil water pressure-moisture mathematical models proposed by Brooks and Corey [26] are given by:

$$\theta(\psi) = \theta_r + (\theta_s - \theta_r) \left(\frac{\psi_d}{\psi} \right)^n \text{ if } \psi \leq \psi_d$$

$$\theta(\psi) = \theta_s \text{ if } \psi > \psi_d$$

$$K(\psi) = K_s \left[\frac{\theta(\psi) - \theta_r}{\theta_s - \theta_r} \right]^{3+2/n} \text{ if } \psi \leq \psi_d$$

$$K(\psi) = K_s \text{ if } \psi > \psi_d$$

$$C(\psi) = n \frac{\theta_s - \theta_r}{|\psi_d|} \left(\frac{\psi_d}{\psi} \right)^{n+1} \text{ if } \psi \leq \psi_d$$

$$C(\psi) = 0 \text{ if } \psi > \psi_d$$

where θ_s is the saturated moisture content [$L^3 L^{-3}$], θ_r is the residual moisture content [$L^3 L^{-3}$], $\psi_d = -\frac{1}{\alpha}$ is the air entry pressure head [L] and $m = 1 - \frac{1}{n}$ is a pore-size distribution index.

ii. *Van Genuchten Model*

Van Genuchten model [27] is the most used characteristic function for moisture content and hydraulic conductivity and presented as follows:

$$\theta(\psi) = \theta_r + \frac{\theta_s - \theta_r}{[1 + |\alpha\psi|^n]^m} \text{ if } \psi \leq 0$$

$$\theta(\psi) = \theta_s \text{ if } \psi > 0$$

$$K(\psi) = K_s \left[\frac{\theta - \theta_r}{\theta_s - \theta_r} \right]^{0.5} \left\{ 1 - \left[1 - \left(\frac{\theta - \theta_r}{\theta_s - \theta_r} \right)^{\frac{1}{m}} \right]^m \right\}^2 \text{ if } \psi \leq 0$$

$$K(\psi) = K_s \text{ if } \psi > 0$$

Ref

27. Van Genuchten, M.T.:A *Closed-form Equation for Predicting the Hydraulic Conductivity of Unsaturated Soils*. Soil Sci. Soc. Am. J. 1980, 44:892–898.

$$C(\psi) = \alpha mn \frac{\theta_s - \theta_r}{[1 + |\alpha\psi|^n]^{m+1}} |\alpha\psi|^{n-1} \text{ if } \psi \leq 0$$

$$C(\psi) = 0 \text{ if } \psi > 0$$

b) Spatial Discretization

An appropriate technique to divided the boundary-value spatial component of Richards' equation from its initial-value temporal variation is the finite element technique and this approach is very simple and practical to use. To build up the finite element algorithm of the pressure head-based Richards' equation, the weak model of the dependent variable and the constitutive relations were approximated utilizing introducing polynomials [28, 29]. It was expected that the pressure driven conductivity just as capacitance differs linearly inside every component [30].

For solving Richards' equation (1) numerically, finite element Galerkin's approach is applied to discretize spatial domain and finite difference method is used for time derivative term. To build up the finite element model, there are M-1 discretized components for M global nodes in the problem domain.

The approximating function is

$$\psi(z, t) \approx \hat{\psi}(z, t) = \sum_{j=1}^M N_j(z) \psi_j(t) \quad (16)$$

where $N_j(z)$ and $\psi_j(t)$ are linear Lagrange basis functions and nodal values of ψ at time t , respectively. The method of weighted residuals is used to set the criteria to solve for the unknown coefficients. In local coordinate space $-1 \leq \xi \leq 1$, the approximating function for each element (e) is $\hat{\psi}^{(e)} = \sum_{i=1}^2 N_i^{(e)}(\xi) \psi_i^{(e)}(t) = \frac{1}{2}(1 - \xi)\psi_1^{(e)}(t) + \frac{1}{2}(1 + \xi)\psi_2^{(e)}(t)$, which we can write in vector form as $\hat{\psi}^{(e)} = (N^{(e)}(\xi))^T \Psi^{(e)}(t)$. The global function (16) becomes:

$$\hat{\psi} = \sum_{e=1}^{M-1} (N^{(e)})^T \Psi^{(e)} = \sum_{e=1}^{M-1} \hat{\psi}^{(e)}$$

The symmetric weak formulation of Galerkin's method applied to (1) yields the system of ordinary differential equations [14]:

$$A(\Psi)\Psi + F(\Psi) \frac{d\Psi}{dt} = q(t) - b(\Psi)$$

where Ψ is the vector of undetermined coefficients corresponding to the values of pressure head at each node, A is the stiffness matrix, F is the storage or mass matrix, q contains the specified Darcy flux boundary conditions and b contains the gravitational gradient component. Over local sub domain element $\Omega^{(e)}$, we have:

$$A^{(e)} = \int_{\Omega^{(e)}} K_s^{(e)} K_r(\hat{\psi}^{(e)}) \frac{dN^{(e)}}{dz} \left(\frac{dN^{(e)}}{dz} \right)^T dz$$

$$b^{(e)} = \int_{\Omega^{(e)}} K_s^{(e)} K_r(\hat{\psi}^{(e)}) \frac{dN^{(e)}}{dz} dz$$

$$F^{(e)} = \int_{\Omega^{(e)}} C(\hat{\psi}^{(e)}) N^{(e)} (N^{(e)})^T dz$$

Here, N^T denotes the transpose of N .

c) *Time Differencing*

Equation (18) can be integrated by the weighted finite difference scheme. We obtain:

$$A(\Psi^{k+\lambda})\Psi^{k+\lambda} + F(\Psi^{k+\lambda}) \frac{\Psi^{k+1} - \Psi^k}{\Delta t^{k+1}} = q(t^{k+\lambda}) - b(\Psi^{k+\lambda})$$

where $\Psi^{k+\lambda} = \lambda\Psi^{k+1} + (1 - \lambda)\Psi^k$, with $0 \leq \lambda \leq 1$ (λ is a weighting parameter) and $k + 1$ denotes current time level.

The time step size to ensure a stable solution will be dependent on the spatial discretization, and for nonlinear equations, there will in general also be a dependency on the form of the solution itself at any given time. Equation (22) is $O(\Delta t)$ accurate, except for $\lambda = \frac{1}{2}$. When $\lambda = \frac{1}{2}$, the discretized scheme (22) corresponds to the Crank–Nicolson scheme.

The system of equations (22) is nonlinear in Ψ^{k+1} , except when $\lambda = 0$, which corresponds to an explicit Euler scheme. When $\lambda > 0$, the scheme becomes implicit. Some iteration or linearization strategy is thus needed to solve the system of nonlinear equations for the implicit case. For $\lambda = 1$, the scheme corresponds to the backward Euler scheme.

III. ITERATIVE METHODS

The system of equations (22) is highly nonlinear because of the nonlinear dependency of hydraulic conductivity K and specific moisture capacity C on ψ . Picard and Newton are the two classical iterative approaches can be applied in the nonlinear system (22) for linearization. Picard method is simpler than Newton and preserves symmetry in the system matrix. Then again, the Newton strategy requires the computation of Jacobian matrix at each iteration and yields a nonsymmetric system. Along these matters, Picard technique is less computational, on a for every cycle premise, than the Newton strategy. The Picard strategy is convergent linearly, whereas, Newton meets quadratically.

a) *Newton Scheme*

Let us Consider

$$\begin{aligned} f(\Psi^{k+1}) \\ = A(\Psi^{k+\lambda})\Psi^{k+\lambda} + F(\Psi^{k+\lambda}) \frac{\Psi^{k+1} - \Psi^k}{\Delta t^{k+1}} \\ - q(t^{k+\lambda}) + b(\Psi^{k+\lambda}) = 0 \end{aligned}$$

Notes

The Newton scheme [3] can be written as:

$$f'(\psi^{k+1,(m)})(\psi^{k+1,(m+1)} - \psi^{k+1,(m)}) = -f(\psi^{k+1,(m)})$$

where the superscripts m and $m + 1$ denote the previous and current iteration levels respectively.

The Jacobian for the system is:

$$\begin{aligned} f'_{ij} &= \lambda A_{ij} + \frac{1}{\Delta t^{k+1}} F_{ij} + \sum_s \frac{\partial A_{is}}{\partial \psi_j^{k+1}} \psi_s^{k+\lambda} \\ &+ \frac{1}{\Delta t^{k+1}} \sum_s \frac{\partial F_{is}}{\partial \psi_j^{k+1}} (\psi_s^{k+1} - \psi_s^k) + \frac{\partial b_i}{\partial \psi_j^{k+1}} \end{aligned}$$

expressed here in terms of ij -th component of the Jacobian matrix $f'(\Psi^{k+1})$.

b) Picard Scheme

Straightforward and simple mathematical expression of Picard iterative method can be derived from (22) by iterating with all linear events of ψ^{k+1} taken at the current iteration level $m + 1$ and all nonlinear events at the previous level m [3]. We get:

$$\begin{aligned} &\left[\lambda A^{k+\lambda,(m)} + \frac{1}{\Delta t^{k+1}} F^{k+\lambda,(m)} \right] (\psi^{k+1,(m+1)} - \psi^{k+1,(m)}) \\ &= -f(\psi^{k+1,(m)}) \end{aligned}$$

By the comparison of the equations (22) and (26), it is observed that Picard technique is an approximation of Newton technique. To assess the overall efficiency of the two linearization techniques, it is very important to know the structural differences of Picard and Newton techniques, such as, Picard linearization produces symmetric and Newton produces a nonsymmetric system matrix. Three derivative terms are needed to calculate in the Newton procedure, as a result, the Newton strategy is more expensive and arithmetically complex than Picard.

IV. METHODOLOGY

The principal objective of this research is to generalize pressure head-based finite element algorithm to handle the nonlinearity, minimize the mass balance errors locally and globally of the flow equation and application of one-dimensional saturated flow conditions for investigating the spatial and temporal discretization affect. This is practiced by linearizing a head-based flow equation with the Picard and Newton iteration techniques. An unusual Galerkin finite element technique is then used to comprehend the linearized definition to acquire the solution of flow problems.

Mass balance errors and computational efficiency are the key factors for the measure of the solution quality. Numerical trials will be introduced to delineate the promising solution execution of the iteration techniques as contrasted and the reference solution which will be made by fine grid resolutions maintain with a tight nonlinear tolerance for the test problems to evaluate the efficiency and robustness and also



compare the computed result with other published footprints. Note that the input tolerance level will affect the accuracy of the numerical solution, within limits imposed by spatial and temporal truncation error.

The exhibition of the calculation is contrasted and two illustrative arrangements of distributed exploratory information, every one of which speaks to an alternate physical situation and is frequently used to approve calculations. In the test examples, the accuracy, mass balance character and iteration efficiency of the pressure head-based model is evaluated with the Picard and the Newton iteration schemes using three different spatial and time-step sizes, and applicability of the resultant solutions, and draw methods to assess the computational work required to achieve the results. Numerical experiments are performed with mass lumping, to appraise the robustness of the approach and investigate the advantages of the methods for improving the efficiency of solutions to Richards' equation.

To enhance the convergence of the nonlinear iterative approaches, dynamic time stepping technique is incorporated in this study. During whenever step, nonlinear convergence tolerance Tol ($= 10^{-4}$) is assigned for both the test examples, alongside a most extreme number of nonlinear iterations denoted by $maxit$ and it is 15. Simulation start with time step size is Δt_0 and proceeds until we arrive at the end of the simulation time T_{max} . Present step size will increase with a predetermined amplification factor Δt_{mag} ($= 1.20$) if the number of iterations is less than another pre-assigned limit of iterations $maxit_1$ ($= 8$) and this process is repetitive until reach the maximum time step size Δt_{max} . Current step size is constant if number of nonlinear iterations are lies between $maxit_1$ and $maxit_2$ ($= 5$) iterations. If the number of nonlinear iterations is less than $maxit_2$, then the simulation step size will reduce by a reduction factor Δt_{red} ($= 0.5$) to assigned minimum step size Δt_{min} . Solution will start recalculate if the convergence is not attaining within the specified maximum number of nonlinear iterations, which is called back-stepping. For both the iterative schemes, the infinity norm [11], $\|\psi^{k+1,(m+1)} - \psi^{k+1,(m)}\| \leq Tol$ is used as the stopping criterion.

A correlation of the overall precision of the numerical outcomes got from various plans is not easy [15]. It is depending upon the objectives such as, global or local comparisons of water pressure or water content, minimum or maximum value of the compared variable, etc. One proportion of a numerical test system is its capacity to preserve global mass over the area of intrigue. Small mass balance error is necessary yet not totally satisfactory essential for a correct solution [4, 15, 31]. To quantify the capacity of the test system to conserve mass, one of the most broadly utilized models for assessing the accuracy of a numerical strategy is the mass balance error (MBE) given by [4]:

$$\text{Mass Balance Error} = 1 - \frac{\text{Total additional mass in the domain}}{\text{Total net flux into the domain}}$$

where the complete extra mass in the space is the distinction between the mass estimated at any moment t and the underlying mass in the area, and the total net flux into the region is the flux balance coordinated in time up to t . In this study, this is determined by the accompanying equation [4]:

Ref

4. Celia, M. A., Bouloutas, E. T., and Zarba, R. L.: *A General mass-conservative numerical solution for the unsaturated flow equation*, Water Resour. Res., 1990, 26(7):1483-1496.

$$MB(t) = \frac{\sum_{i=1}^{E-1} (\theta_i^{k+1} - \theta_i^0)(\Delta z) + (\theta_0^{k+1} - \theta_0^0) \left(\frac{\Delta z}{2} \right) + (\theta_E^{k+1} - \theta_E^0) \left(\frac{\Delta z}{2} \right)}{\sum_{j=1}^{k+1} \{ (q_o^j - q_N^j)(\Delta t) \}} \quad (27)$$

with $N = E + 1$ nodes $\{z_0, z_1, z_2, \dots, z_E\}$, and constant nodal spacing Δz is considered and q_0 and q_N being boundary fluxes evaluated from the finite element equations related with the boundary modes z_0 and z_N .

To solve the linearized system of equations, a main drawback of the Newton scheme is insufficiency of linear solvers for large, sparse non symmetric systems. This is not true anymore, as at present accessible form conjugate gradient-type algorithms for handling non symmetric systems have gotten progressively steady and effective. In this work, bi-conjugate gradient stabilized algorithm (BICGSTAB) is used to solve the linear systems. For the symmetric system produced by Picard linearization, incomplete Cholesky conjugate gradient strategy (ICCG) is joined. For all experiments, where ICCG, BICGSTAB, iterative solver, the linear solver boundaries *tolcg* (convergence tolerance 10^{-10}) and *maxitcg* (maximum number of linear iterations is 1000) was assigned. Soil moisture properties are evaluated by analytical differentiation.

Hydrological model CATHY (CATchmentHYdrology) [11, 32], where the surface module settles the one-dimensional diffusion wave condition and the subsurface module solves the three-dimensional Richards' equation, is used for all runs. All simulations were executed on a Dell Inspiron 2.56-GHz laptop computer.

V. RESULTS AND DISCUSSIONS

Two challenging one-dimensional test examples are considered to validate the algorithm and to compare the accuracy of the numerical solution of Richards' equation by the CATHY model. Time dependent boundary conditions with a sharp moisture front that infiltrates into the soil column [10, 16, 33] is the first test problem and the second test case involves flow into a layered soil with variable initial conditions [33, 34, 35].

a) Test problem 1

This problem considers a soil column of 2 m deep with the initial pressure head distribution is $\psi(z, 0) = z - 2$. At the bottom of the column, a water table boundary condition (i.e., $\psi(0, t) = 0$) is imposed, while a time-dependent Dirichlet condition

$$\psi(2, t) = \begin{cases} -0.05 + 0.03 \sin\left(\frac{2\pi t}{100000}\right) & \text{if } 0 < t \leq 100000 \\ 0.1 & \text{if } 100000 < t \leq 180000 \\ -0.05 + 2952.45 e^{-\frac{t}{18204.8}} & \text{if } 180000 < t \leq 300000 \end{cases}$$

is applied at the top boundary which is presented in Figure 1. The soil hydraulic properties are described by the van Genuchten model. The soil parameters are $\theta_s = 0.410$, $\theta_r = 0.095$, $\alpha = 1.9/m$, $n = 1.31$ and $K_s = 0.062 \text{ m/day}$.

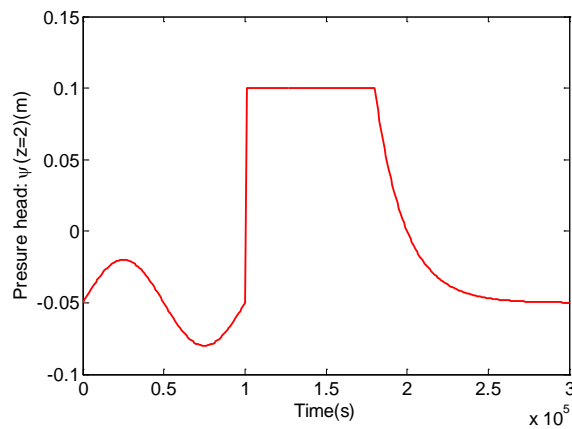


Figure 1: Dirichlet boundary condition imposed at the top of the soil column for Test problem 1

The Dirichlet boundary condition leads to significant ponding between 100000 sand 200000 s, and as will be found in the outcomes, this kind of boundary condition, leading in coupled groundwater water representation, is a wellspring of huge trouble in the iterative techniques.

Attributes of such soil compare to an unconsolidated clay loam with a nonuniform grain size circulation [36]. Antecedent experiment [37] completed a comparative correlation utilizing a moisture-based type of Richards' equation and an alternate experiment that doesnot include time-differing boundary conditions with surface ponding.

Due to the positive value of pressure head in the second period of simulation time ($100000 < t \leq 180000$ s), to achieve the numerical convergence is very challenging for any algorithm. In light of unexpected increment of the upper Dirichlet boundary condition to a positive estimation of 0.1 m, it makes a sharp moisture front that infiltrates into the soil section. Toward the start of the third time frame ($t > 180000$ s) ponding diminishes exponentially, arriving at asymptotically a last worth -0.05 m, and before the finish of the simulation the whole section is near tofull saturation.

The moisture retention curve is monotonic with a point of inflection that gives the moisture capacity function its typical shape. The soil moisture retention curves for this test problem using the van Genuchten model are represented in Figure 2.

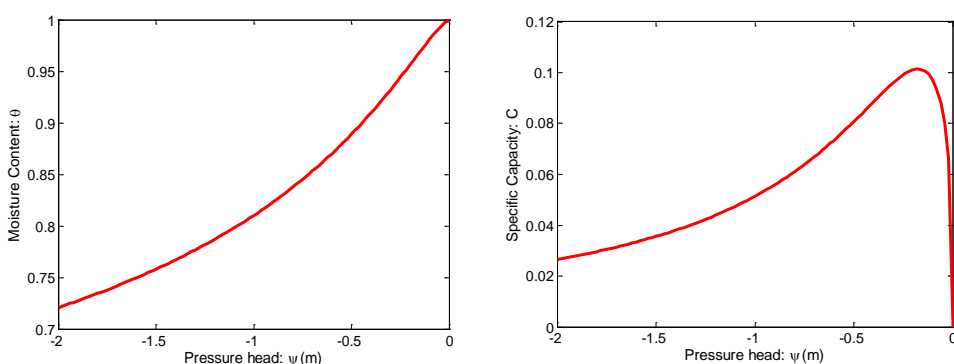


Figure 2: Soil moisture characteristic curves for Test problem 1

In order to assess the robustness and efficiency of the method, we used three set of grid sizes, i.e., $\Delta z = 0.004 \text{ m}$, 0.008 m and 0.04 m and each grid discretization is simulated with three temporal sizes $\Delta t_{max} = 1000 \text{ s}$, 100 s and 10 s .

The computed pressure head profiles at various meshing obtained with a small tolerance (10^{-4} m) are displayed in Figure 3. These solutions are very similar to those reported in the literature [10, 16, 33]. Figure 3 shows the initial conditions and pressure head solution profiles at three different times (e.g., 0 s , 35000 s , 155000 s and 300000 s). It is evident that the solution profiles are affected by the spatial resolutions. The red profiles, which falls inside the ponding time frame, shows the abundance water that structures at the soil surface and the fairly sharp moisture front that is produced.

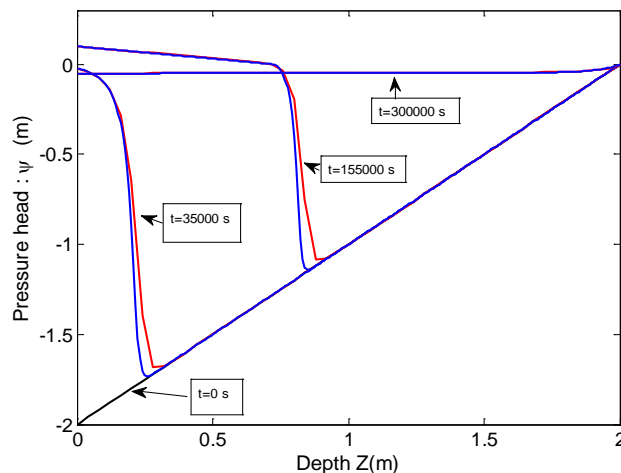


Figure 3: Pressure head profiles at different times for $\Delta z = 0.04 \text{ m}$ (red) and $\Delta z = 0.008 \text{ m}$ (blue) of Test problem 1

Adaptive time stepping algorithm is applied to the iteration techniques Newton and Picard for all vertical discretizations and three different time stepping scales for investigating the step size behavior. We discovered generally striking here the altogether different conduct between the Newton and Picard methodologies during the ponding time frame. Though the Newton model is compelled to make extremely little step sizes just at the absolute starting point and end of the ponding time frame, the Picard plot needs to arrange a wide scope of step sizes all through the ponding time range, and surely for the $\Delta t_{max} = 1000 \text{ s}$ case, it never accomplishes this most extreme incentive during ponding, for any of the vertical grid resolutions. Small time step size is observed from 100000 s to 200000 s , as ponding progressively diminishes to zero. Step size is quickly increasing and reaches maximum allowable time step size 1000 s in the simulation period 200000 s to 300000 s for both iteration schemes. This demonstrates simpler nonlinear solver conditions because of smoother infiltration fronts and surface conditions that are no longer fully saturated. Compelling an iteration scheme to take extremely small time steps for prolonged periods during a simulation can represent a massive computational trouble for subsurface solvers. The time stepping behavior of Picard and Newton can be found in the Figure 4 for $\Delta z = 0.008 \text{ m}$ and 0.04 m cases with various time step sizes.

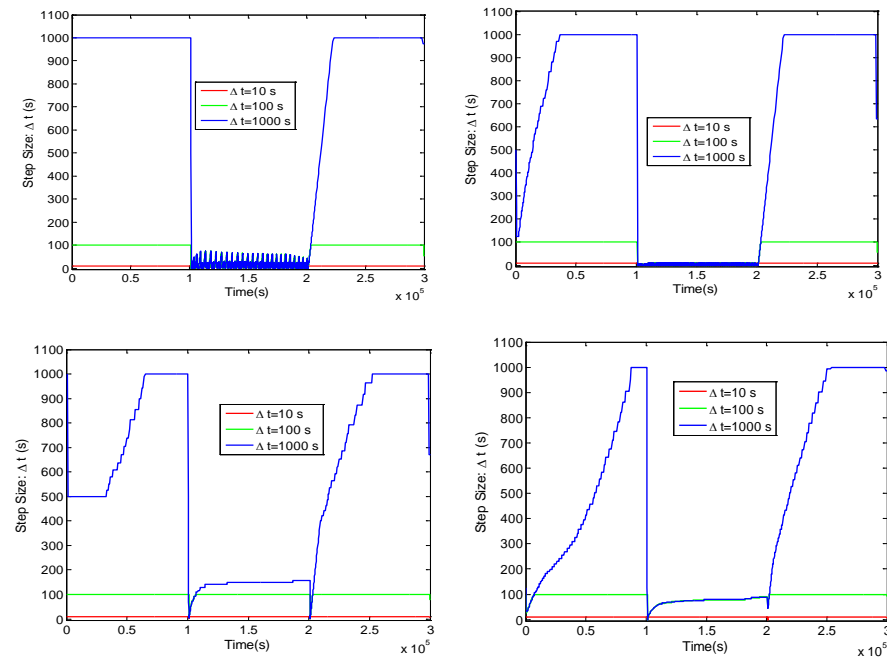


Figure 4: Dynamic time stepping behavior of Picard (top row) and Newton (bottom row) schemes for $\Delta z = 0.04 \text{ m}$ (left) and $\Delta z = 0.008 \text{ m}$ (right) of Test problem 1

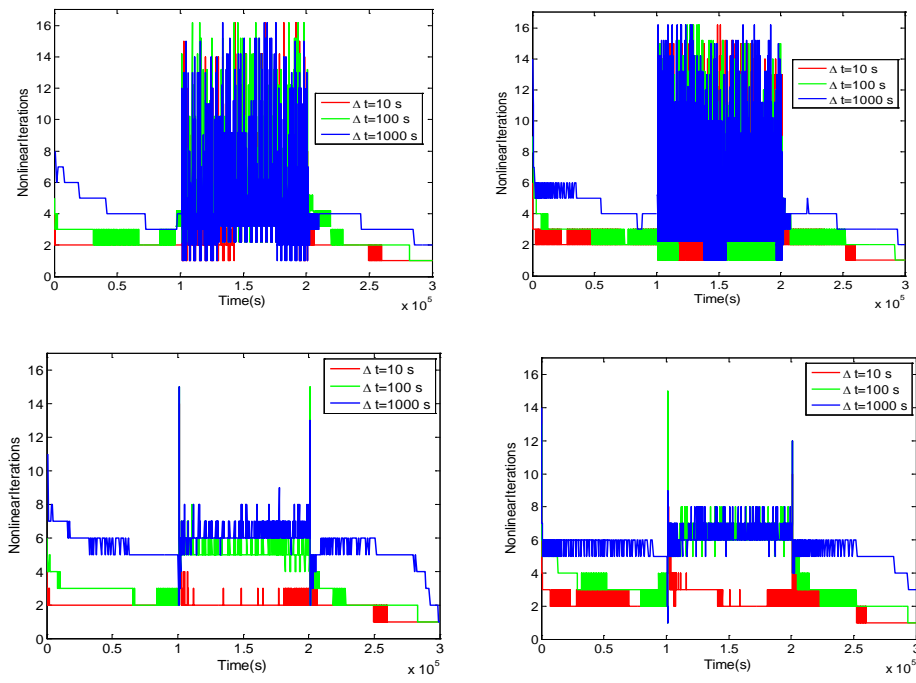


Figure 5: Nonlinear convergence behavior of Picard (top row) and Newton (bottom row) schemes for $\Delta z = 0.04 \text{ m}$ (left) and $\Delta z = 0.008 \text{ m}$ (right) of Test problem 1

Graphical representation of convergence nature on the basis of number of nonlinear iterations required at each step of Picard and Newton iteration schemes are shown in the Figure 5. Here, we observed that a smoother transition into and out of the ponding period, and without the need for time step adaptation. Solver needs to negotiate a wide range of iteration to achieve converge.

Using Picard and Newton techniques, cumulative mass balance error (CMBE) plot is presented in the Figure 6 for all temporal discretizations. The mass balance error almost closes to zero with the exception of a couple of cases around 100000 s implied that the accurate solution is ensured. Nonlinear iteration, time stepping and CMBE behavior of $\Delta z = 0.004 \text{ m}$ case is not presented graphically as they are almost same as for $\Delta z = 0.008 \text{ m}$. Note that Newton method cannot converge for $\Delta t = 100 \text{ s}$ and 1000 s for grid spacing $\Delta z = 0.004 \text{ m}$.

The computational statistics of the methods under all the cases are summarized in Table 1 and Table 2. The performance indicators are the total number of iterations, cumulative mass balance error, the average number of Picard and Newton iterations taken at each time step, the number of back stepping occurrences i.e., failure of Picard or Newton to converge within the assigned maximum number of iterations, the number of linear solver failures and the computational time (CPU). Examining more closely both iterative results, we note that Newton scheme resulted in significantly fewer back-stepping occurrences. Graphical results and statistics of the simulation clearly indicate that the technique is adequate.

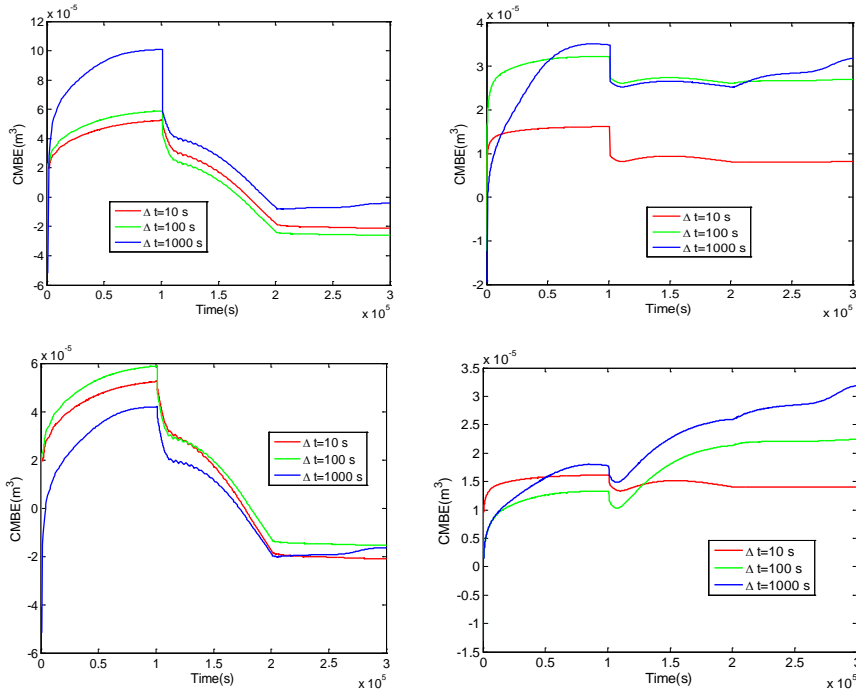


Figure 6: Cumulative mass balance error behavior of Picard (top row) and Newton (bottom row) schemes for $\Delta z = 0.04 \text{ m}$ (left) and $\Delta z = 0.008 \text{ m}$ (right) of Test problem 1

Another precision of simulation is assessed by the root mean squared error (RMSE) as for the reference solution which is made utilizing very fine grid with very small nonlinear tolerance. Errors are measured at three different times, explicitly, at 35000 s, 155000 s, and 300000 s for all the temporal discretizations of Picard and Newton techniques (Table 3). We have appeared (Figure 7) that the normal errors are most noteworthy at the coarsest spatial and temporal discretizations, and the pinnacle errors spread with the moisture front that is moving downwards into the soil. Furthermore, Picard scheme gives little higher errors than Newton scheme and sharp increment in absolute error in the range of ponding time is observed. Choice of the

discretization method of spatial and temporal domain has a great impact on handling soil properties, as a result, numerical accuracy can be affected significantly including the stability and rate of convergence of the numerical scheme.

Table 1: Computational statistics of Picard scheme for Test problem 1

$\Delta t_{max}(s) \rightarrow$	10			100			1000		
$\Delta z (m) \rightarrow$	0.04	0.008	0.004	0.04	0.008	0.004	0.04	0.008	0.004
MBE (m^3)	-2.11e-5	8.12e-6	8.44e-6	-2.13e-5	9.85e-6	4.95e-6	-2.11e-5	8.12e-6	8.44e-6
No. of time step	42583	136622	186242	303006	364601	403462	42583	136622	186242
NL Ite/Step	2.22	2.44	2.37	1.43	1.65	1.70	2.22	2.44	2.37
Back step	1084	7911	11419	367	6290	9564	1084	7911	11419
Solver failures	0	0	0	0	0	0	0	0	0
CPU (s)	5546	80729	202349	3679	69892	74496	3055	7790	183895

* NL Ite=Nonlinear Iteration

Notes

Table 2: Computational statistics of Newton scheme for Test problem 1

$\Delta t_{max}(s) \rightarrow$	10			100			1000		
$\Delta z (m) \rightarrow$	0.04	0.008	0.004	0.04	0.008	0.004	0.04	0.008	0.004
MBE (m^3)	-2.09e-5	1.40e-5	5.90e-6	-1.52e-5	2.24e-5	Div	-1.65e-5	3.19e-5	Div
No. of time step	30149	30247	30266	3187	3737	Div	1281	2237	Div
NL Ite/Step	1.86	2.05	2.08	3.38	4.26	Div	5.58	5.93	Div
No. of back step	6	16	14	7	12	Div	15	22	Div
Solver failures	0	2	1	0	1	Div	1	3	Div
CPU (s)	6949	52378	70347	1385	11303	Div	911	7790	Div

* Div=Divergent

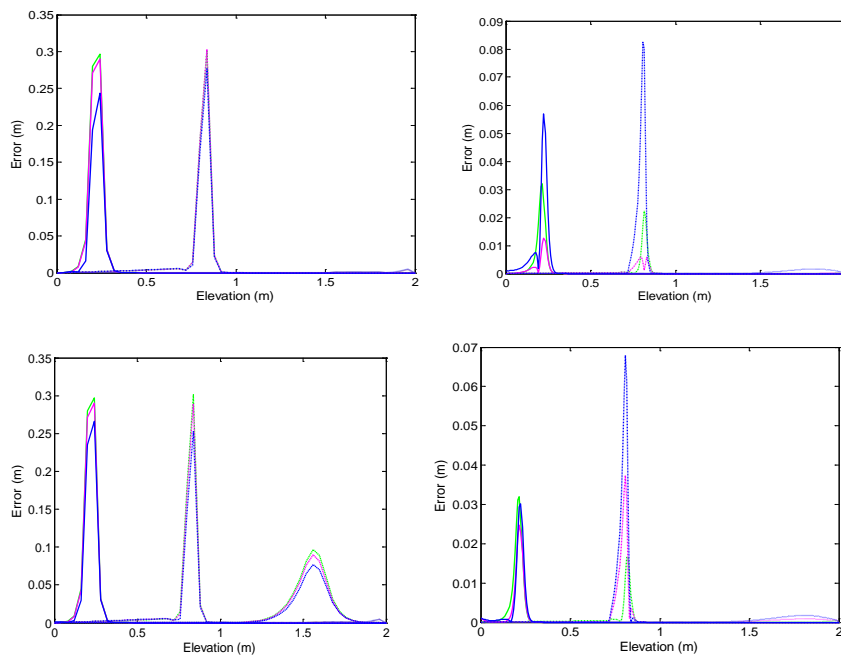


Figure 7: RMSE behavior of Picard (top row) and Newton (bottom row) schemes for $\Delta z = 0.04 m$ (left) and $\Delta z = 0.008 m$ (right) of Test problem 1. Errors at 35000s, 155000s and 300000s are marked by solid, dash-dotted, dashed lines with green, magenta, blue colors respectively

Table 3: RMSE of Picard and Newton schemes for Test problem 1

Δz (m)	Δt_{max} (s)	Time (s) →	35000	155000	300000
		Method ↓			
0.04	10	Picard	5.76e-2	4.93e-2	9.33e-4
		Newton	5.76e-2	4.94e-2	9.33e-4
	100	Picard	5.61e-2	4.98e-2	9.37e-4
		Newton	5.62e-2	4.73e-2	9.19e-4
	1000	Picard	4.38e-2	4.54e-2	9.15e-4
		Newton	5.01e-2	4.12e-2	9.05e-4
0.008	10	Picard	4.20e-3	2.50e-3	6.62e-5
		Newton	4.20e-3	1.90e-3	6.89e-5
	100	Picard	1.50e-3	9.80e-3	9.69e-5
		Newton	3.20e-3	4.50e-3	3.32e-4
	1000	Picard	6.60e-3	1.00e-3	5.98e-4
		Newton	3.37e-3	8.10e-3	6.36e-4

b) Test problem 2

The simulations of this test case with different layer thicknesses with the heterogeneity in the soil moisture retention curves, represented with the Brooks–Corey model. This case involves vertical drainage from initially saturated conditions. At time $t = 0$ s, the pressure head at the base of the column is reduced from 2 m to 0 m. During the subsequent drainage, a no-flow boundary condition is applied to the top of the soil column. These forcing conditions lead to the development of a sharp discontinuity in the moisture content occurs at the interface between two material layers [33, 34, 35]. This type of problem provides a rigorous test case for a numerical algorithm and is well suited for the analysis of numerical convergence and efficiency.

During downward draining, the middle coarse soil tends to restrict drainage from the upper fine soil, and high saturation levels are maintained in the upper fine soil for a considerable period of time. The hydraulic properties of the soils are given in Table 4. The soil profile is Soil 1 for $0 < z < 60$ cm and 120 cm $< z < 200$ cm and Soil 2 for 60 cm $< z < 120$ cm.

Table 4: Soil hydraulic properties used in Test problem 2

Parameters	Soil 1	Soil 2
θ_s	0.35	0.35
θ_r	0.07	0.035
α (cm ⁻¹)	0.0286	0.0667
n	1.5	3.0
K_s (cm/s)	9.81×10^{-5}	9.81×10^{-3}

The soil moisture curves of the moisture content (θ) and specific moisture capacity (C) are evaluated by the Brooks–Corey model (Figure 8). The shape of the soil moisture capacity is very sharp near the saturation implies the rigorous complexities are encountered when the analytical differentiation of fluid content is used. As a consequence, numerical accuracy can be affected significantly. To handle such difficulties efficiently, proper choice of grid resolution and temporal discretization is required for heterogeneous porous media.

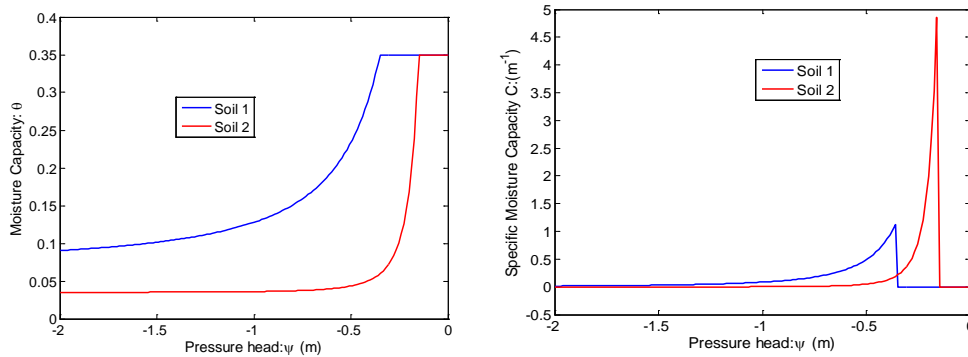


Figure 8: Soil moisture characteristic curves for Test problem 2

To compare the performance of the algorithm, simulations are performed on two fine mesh of 300 and 150 elements and a coarser mesh of 50 elements with three time step sizes ($\Delta t_{max} = 10\text{ s}$, 100 s and 1000 s) via dynamic time stepping control for nonlinear iterations with mass lumping. The algorithm is used to simulate the experiment and the comparison of water saturation prediction after 1050000 s is depicted in Figure 9, which is similar to those presented in the published result [33, 34, 35]. Some oscillations are produced in the middle coarse soil in the solution profile, as our expectation. These oscillations have been attributed to insufficient spatial resolution.

The simulations conducted with small grid spacing produce more acceptable results in that the overall shape of the soil hydraulic characteristic. However, that use of even smaller grid spacing may not significantly improve the simulation results. It is recommended that the computed saturation is sensitive about grid spacing.

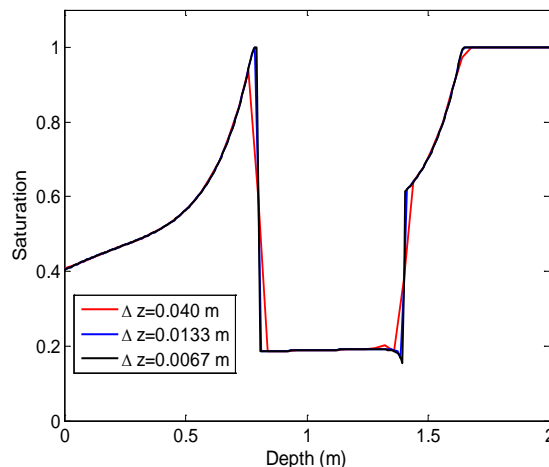


Figure 9: Saturation predictions after 1050000 s for different spatial discretizations of Test problem 2

Adaptive time stepping behavior (Figure 10), nonlinear iterations per time step (Figure 11) and cumulative mass balance error (Figure 12) are presented graphically for the case $\Delta z = 0.04\text{ m}$ and $\Delta z = 0.0133\text{ m}$. Almost similar results are recorded for 150 and 300 elements. So, in the figure analysis on the basis of the mentioned factors are excluded for 300 elements. Time stepping plots shows that Picard scheme has to face very little trouble at $2 \times 10^5\text{ s}$, whereas Newton scheme is highly affected during the

Notes

simulation for $\Delta t_{max} = 100$ s and 1000 s. But note that, the large time step size speedup to complete the simulation. Convergence plots demonstrated that, Picard and Newton techniques need only one iteration during entire simulation for $\Delta t_{max} = 10$ s. There are some differences are observed for other time scales as well grid spacing. Cumulative mass balance errors are almost approaching to zero. This implies that the numerical results are strictly maintained accuracy. Table 5 and 6 summarized the simulation statistics for Picard and Newton iteration methods respectively. The mass balance error at any given time step is calculated as the absolute difference between the changes in water storage during that time step. In this test case, Newton technique needs many back-stepping to achieve the convergence for all spatial and temporal discretizations. RMSE evaluated with respect to the surrogate exact solution with very small nonlinear tolerance. Errors are measured at the three different times, specifically, at 250000 s, 550000 s, and 1050000 s for all the temporal discretizations of Picard and Newton techniques (Table 7).

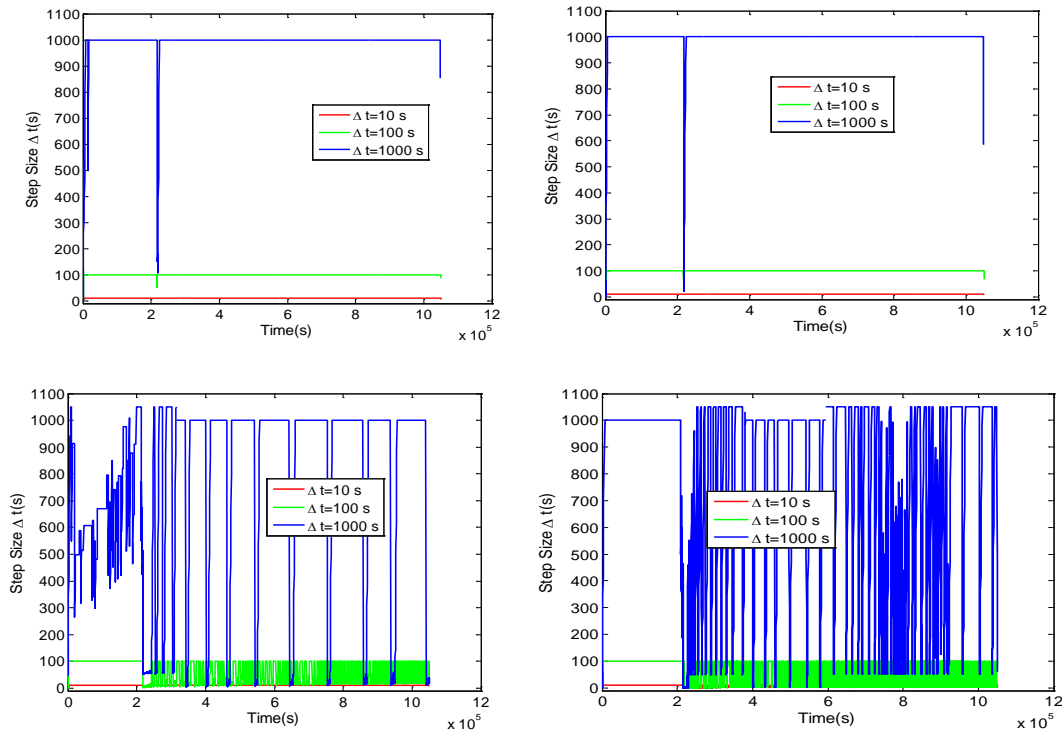
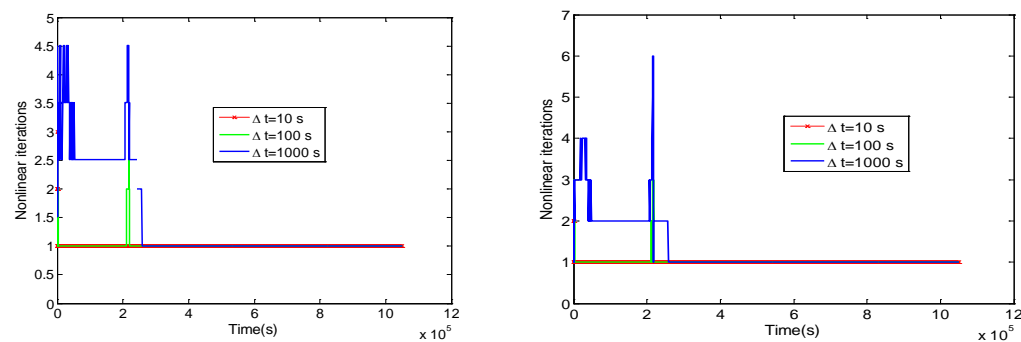


Figure 10: Dynamic time stepping behavior of Picard (top row) and Newton (bottom row) schemes for $\Delta z = 0.04$ m (left) and $\Delta z = 0.0133$ m (right) of Test problem 2



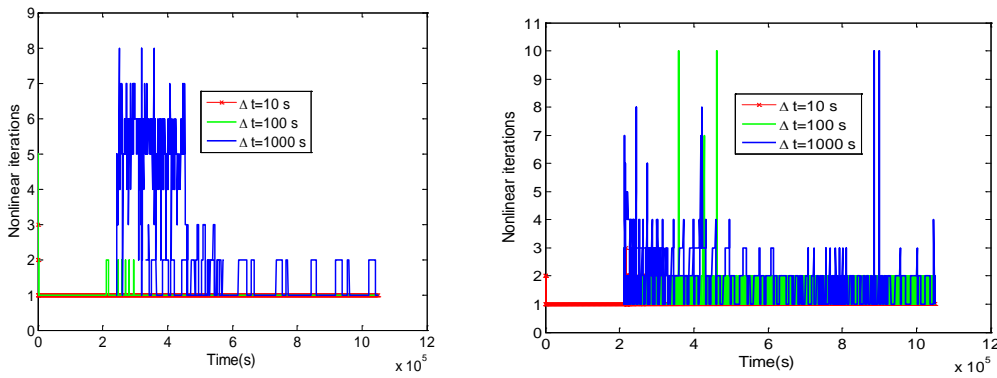


Figure 11: Nonlinear convergence behavior of Picard (top row) and Newton (bottom row) schemes for $\Delta z = 0.04 \text{ m}$ (left) and $\Delta z = 0.0133 \text{ m}$ (right) of Test problem 2

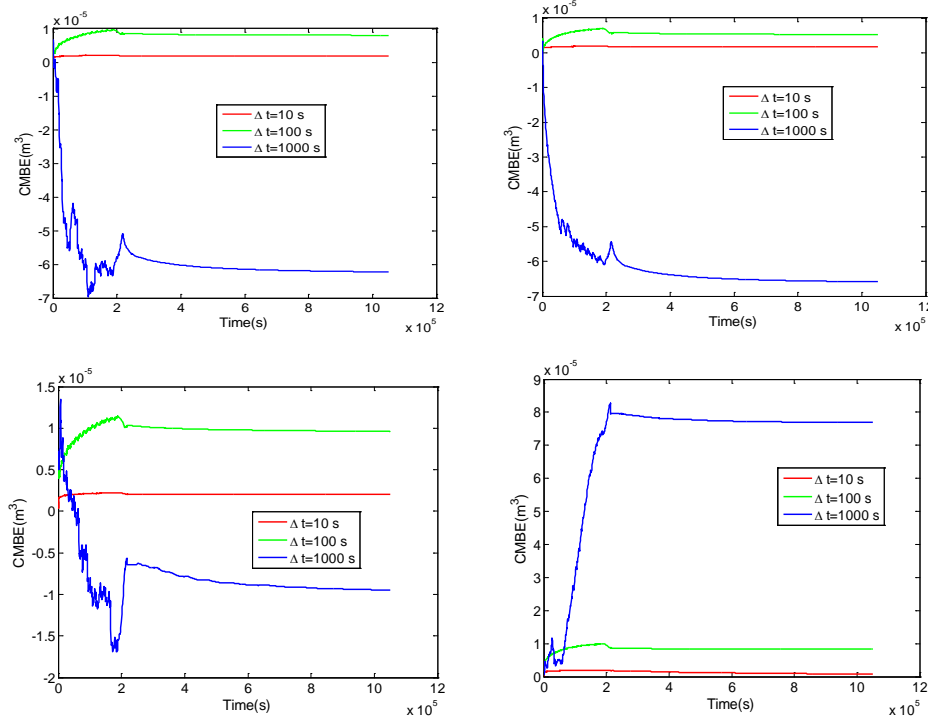


Figure 12: Cumulative mass balance error behavior of Picard (top row) and Newton (bottom row) schemes for $\Delta z = 0.04 \text{ m}$ (left) and $\Delta z = 0.0133 \text{ m}$ (right) of Test problem 2

Table 5: Computational statistics of Picard scheme for Test problem 2

$\Delta t_{max}(s) \rightarrow$	10			100			1000		
$\Delta z (m) \rightarrow$	0.04	0.0133	0.0067	0.04	0.0133	0.0067	0.04	0.0133	0.0067
MBE (m^3)	1.88e-6	1.72e-6	1.43e-6	8.03e-6	0.0067	3.11e-6	-6.23e-5	6.59e	-7.44e-5
No. of time step	105051	105051	105051	10566	5.28e-6	10556	1146	43602	1136
NL Ite/Step	1.00	1.00	1.00	1.04	1.03	7.56	1.62	3.62	1.58
No. of back step	15	15	15	20	1.03	16	29	28	25
Solver failures	0	0	0	0	19	0	0	0	0
CPU (s)	6449	14034	47528	767	2506	4050	134	631	966

Table 6: Computational statistics of Newton scheme for Test problem 2

$\Delta t_{max}(s) \rightarrow$	10			100			1000		
$\Delta z (m) \rightarrow$	0.04	0.0133	0.0067	0.04	0.0133	0.0067	0.04	0.0133	0.0067
MBE (m^3)	2.20e-6	7.15e-7	7.32e-7	9.59e-6	8.26e-6	7.63e-6	-9.45e-6	7.69e-5	8.59e-5
No. of time step	106217	240041	371587	29024	79014	143872	11137	43602	86856
NL Ite/Step	1.06	3.07	3.10	3.05	3.38	3.53	3.55	3.62	3.65
No. of back step	663	49640	77980	5972	18698	36050	2682	11287	22697
Solver failures	0	0	0	0	19	0	0	0	0
CPU (s)	14945	416403	1340	31101	145679	168846	11400	74944	367914

Table 7: RMSE of Picard and Newton schemes for Test problem 2

$\Delta z (m)$	$\Delta t_{max} (s)$	Time (s) →	250000	550000	1050000
		Method ↓			
0.04	10	Picard	4.70e-3	3.70e-3	3.60e-3
		Newton	5.30e-3	3.70e-3	3.60e-3
	100	Picard	4.70e-3	3.70e-3	3.60e-3
		Newton	5.20e-3	3.90e-3	3.80e-3
	1000	Picard	4.60e-3	3.70e-3	3.60e-3
		Newton	5.50e-3	3.30e-3	3.70e-3
0.0133	10	Picard	1.10e-3	1.00e-3	8.21e-4
		Newton	1.10e-3	1.30e-3	8.95e-4
	100	Picard	1.10e-3	1.00e-3	8.21e-4
		Newton	1.30e-3	1.00e-3	7.72e-4
	1000	Picard	4.60e-3	3.70e-3	3.60e-3
		Newton	1.10e-3	9.83e-4	8.08e-4

VI. CONCLUSIONS

A finite element algorithm is introduced to solve the Richards' equation for one-dimensional flow problems in variably saturated soils. Specifically, the problem of mass-balance errors is handled, which is in reality a pressing problem for the simulation of such highly nonlinear phenomena as the infiltration into soil column and drainage through layered soil from initially saturated condition. The effectiveness of the algorithm is demonstrated by compare with published results. The conduct of various techniques for solution estimates and adaptive time stepping were experimented for Richards' equation model. Time step adaptation is essential to accomplish sensible figuring execution in reasonable uses of Richards' equation. Head based Picard and

Newton iteration schemes are compared, where three step-time sizes are implemented for each of three different spatial discretizations. It is demonstrated that both iterative schemes are mass conservative and efficient in terms of nonlinear iteration. For the most part, large time-step size requires modest number of iterations to converge the solution, however, Newton scheme is diverge for drainage problem, as well as significantly many back-stepping occurred. So, the size of the time step can be constrained by the convergence of the iterative scheme for simulating strong nonlinearities. Coarse grid spacing is caused for numerical oscillations for the both test experiments. Therefore, time step size and/ or grid size are the influential factors for the numerical simulation of variably saturated flows. The model presents tremendous mass balance property over whole spatial and temporal mesh for the problems of infiltration fronts and drainage problems. The accomplishment of the finite element algorithm in simulating an assortment of problems leads to confidence in its applicability to many dynamically saturated flow problems for its advantageous flexibility. Further research is needed in the development of multidimensional finite element model for solving problem in saturated-unsaturated regions without special treatment of fluid content discontinuities in heterogeneous porous media.

ACKNOWLEDGMENTS

This research has been carried out with the financial support of the SUST Research Centre, Shahjalal University of Science & Technology, Sylhet (Project Code: PS/2017/26), Bangladesh.

REFERENCES RÉFÉRENCES REFERENCIAS

1. Miller, C. T., Williams, G. A., Kelly, C. T., and Tocci, M. D.: *Robust solution of Richards' equation for nonuniform porous media*. Water Resour. Res., 1998, 34:2599-2610.
2. Huyakorn, P. S., and G. F. Pinder: *Computational Methods in Subsurface Flow*, Academic, San Diego, Calif, 1983.
3. Paniconi, C., Aldama, A. A., and Wood, E. F.: *Numerical evaluation of iterative and noniterative methods for the solution of the nonlinear Richards' equation*. Water Resour. Res., 1991, 27:1147-1163.
4. Celia, M. A., Bouloutas, E. T., and Zarba, R. L.: *A General mass-conservative numerical solution for the unsaturated flow equation*, Water Resour. Res., 1990, 26(7):1483-1496.
5. Abriola, L.M., and J. Lang, J. R.: *Self-adaptive finite element solution of the one dimensional unsaturated flow equation*. Int. J. Numer. Methods Fluids, 1990, 10:227-246.
6. Grifoll, J., and Cohen, Y.: *A front-tracking numerical algorithm for liquid infiltration into nearly dry soils*. Water Resour. Res., 1999, 35:2579 – 2585.
7. Tocci, M. D., Kelley, C. T., and Miller, C. T.: *Accurate and economical solution of the pressure-head form of Richards' equation by the method of lines*. Adv. Water Resour., 1997, 20(1):1-14.
8. Williams, G.A., and Miller, C.T.: *An evaluation of temporally adaptive transformation approaches for solving Richards' equation*. Adv. Water Resour., 1999, 22(8):831-840.

9. Kavetski, D., Binning, P., and S. W. Sloan: *Adaptive time stepping and error control in a mass conservative numerical solution of the mixed form of Richards equation*. *Adv. Water Resour.*, 2001, 24:595-605.
10. Kavetski, D., Binning, P., and Sloan, S. W.: *Noniterative time stepping schemes with adaptive truncation error control for the solution of Richards' equation*. *Water Resour. Res.*, 2002, 38(10):1211-1220.
11. Paniconi, C., and Putti, M.: *A comparison of Picard and Newton iteration in the numerical solution of multidimensional variably saturated flow problems*. *Water Resour. Res.*, 1994, 30:3357-3374.
12. Fassino, C., and Manzini, G.: *Fast-secant algorithms for the non-linear Richards' Equation*. *Commun. Numer. Methods Eng.*, 1998, 14:921-930.
13. Bergamaschi, L., and Putti, M.: *Mixed finite elements and Newton-type linearizations for the solution of Richards' equation*. *Int. J. Numer. Methods Eng.*, 1999, 45:1025-1046.
14. Jones, J. E., and Woodward, C. S.: *Preconditioning Newton-Krylov methods for variably saturated flow, in XIII International Conference on Computational Methods in Water Resources*, edited by G. F. Pinder, 101-106, A. A. Balkema, Brookfield, Vt., 2000.
15. Lehmann, F., and Ackerer, P. H.: *Comparison of iterative methods for improved solutions of the fluid flow equation in partially saturated porous media*. *Transp. Porous Media*, 1998, 31:275-292.
16. D'Haese, C. M. F., Putti, M., Paniconi, C., and Verhoest, N. E. C.: *Assessment of adaptive and heuristic time stepping for variably saturated flow*. *Int. J. Numer. Methods Fluids*, 2007, 53:1173-1193.
17. Forsyth, P. A., Wu, Y. S. and Pruess, K.: *Robust numerical methods for saturated-unsaturated flow with dry initial conditions in heterogeneous media*. *Adv. Water Resour.*, 1995, 18:25-38.
18. Milly, P. C. D.: *A mass-conservative procedures for time-stepping in models of unsaturated flow*. *Adv. Water Resour.*, 1985, 8:32-36.
19. Pan, L., Warrick, A. W., and Wierenga, P. J.: *Finite element methods for modeling water flow in variably saturated porous media: numerical oscillation and mass-distributed schemes*. *Water Resour. Res.*, 1996, 32:1883-1889.
20. Hills, R. G., Porro, I., Hudson, D. B., and Wierenga, P. J.: *Modeling of one dimensional infiltration into very dry soils: 1. Model development and evaluation*. *Water Resour. Res.*, 1989, 25: 1259-1269.
21. Mansell, R.S., Liwang Ma., Ahuja, L.R., and Bloom, S.A.: *Adaptive Grid Refinement in Numerical Models for Water Flow and Chemical Transport in Soil: A Review*. *Vadose Zone Journal*, 2002, 1:222-238.
22. Diersch, H. J. G., and Perrochet, P.: *On the primary variable switching technique for simulating unsaturated-saturated flows*. *Adv. Water Resour.*, 1999, 23:271-301.
23. Celia, M. A. and Binning, P.: *A mass conservative numerical solution for two-phase flow in porous media with application to unsaturated flow*. *Water Resour. Res.*, 1992, 28(10): 281-928.
24. Huang K, Mohanty, B., and van Genuchten M.: *A new convergence criterion for the modified iteration method for solving the variably saturated flow equation*. *J. Hydrol.*, 1996, 178:69 -91.

25. Hao, X., Zhang, R, and Kravchenko, A.: *A mass-conservative switching method for simulating saturated-unsaturated flow*. *J. Hydrol.*, 2005, xx:1-12.
26. Brooks, R.H.; Corey, A.T. :*Properties of porous media affecting fluid flow*. *J. Irrig. Drain. Div. Am. Soc. Civ. Eng.* 1966, 92:61–88.
27. Van Genuchten, M.T.:*A Closed-form Equation for Predicting the Hydraulic Conductivity of Unsaturated Soils*. *Soil Sci. Soc. Am. J.* 1980, 44:892–898.
28. Allen, M.B., Murphy, C.L.: *A finite element collocation method for variably saturated flow in two space dimension*. *Water Resour. Res.* 1986, 3(11):1537-1542.
29. Zadeh, K. S., Shah, S.B.: *Mathematical modeling and parameter estimation of axonal cargo transport*. *J. Comput. Neurosci.* , 2010, 28(3):495–507.
30. Zadeh, K. S.: *Parameter estimation in flow through partially saturated porous materials*. *J. Comput. Phys.*, 2008, 227(24):10243–10262.
31. Rathfelder, K., Abriola, L.M.: *Mass conservative numerical solutions of the head-based Richards' equation*. *Water Resour. Res.*, 1994, 30(9):2579–86.
32. Camporese, M.; Paniconi, C.; Putti, M.; Orlandini, S.: Surface-subsurface flow modeling with path-based runoff routing, boundary condition-based coupling, and assimilation of multisource observation data. *Water Resour. Res.* 2010, 46, W02512
33. Casulli, V.; Zanolli, P.:*A nested Newton-type algorithm for finite volume methods solving Richards' equation in mixed form*. *SIAM J. Sci. Comput.* 2010, 32:2255–2273.
34. McBride, D.; Cross, M.; Croft, N.; Bennett, C.; Gebhardt, J.:*Computational modeling of variably saturated flow in porous media with complex three-dimensional geometries*. *Int. J. Numer. Methods Fluids* 2006, 50:1085–1117.
35. Marinelli, F.; Durnford, D.S. *Semi analytical solution to Richards' equation for layered porous media*. *J. Irrig. Drain. Eng.*, 1998, 124: 290–299.

Notes